BMB
reports

Suppression of MED19 expression by shRNA induces inhibition of cell proliferation and tumorigenesis in human prostate cancer cells

Xingang Cui[1], Danfeng Xu[1,], Chao Lv[1], Fajun Qu[1], Jin He[2], Ming Chen[1], Yushan Liu[1], Yi Gao[1], Jianping Che[1], Yacheng Yao[1] & Hongyu Yu[2]*

[1]Urology Department of Surgery, [2]Pathology Department, Changzheng Hospital Affiliated to the Second Military Medical University, Shanghai, People's Republic of China

MED19 is a member of the Mediator that plays a key role in the activation and repression of signal transduction or the regulation of transcription in carcinomas. To tested the functional role of MED19 in human prostate cancer, we downregulated MED19 expression in prostate cancer cells (PC-3 and DU145) by lentivirus-mediated short hairpin (shRNA), and analyzed the effect of inhibition of MED19 on prostate cancer cell proliferation and tumorigenesis. The *in vitro* prostate cancer cell proliferation, colony formation, and *in vivo* tumor growth in nude mice xenografts was significantly reduced after the downregulation of MED19. Knockdown of MED19 caused S-phase arrest and induced apoptosis via modulation of Bid and Caspase 7. It was suggested that MED19 serves as a novel proliferation regulator that promotes growth of prostate cancer cells. [BMB reports 2011; 44(8): 547-552]

INTRODUCTION

Prostate cancer is the most commonly diagnosed malignancy and the second leading cause of cancer-related deaths in the Western male population (1). It is estimated that approximately 27,000 victims die of prostate cancer each year, although advances in early detection and treatment have reduced mortality these years (2). Moreover, there is a significant number of men who require systemic therapy and ongoing surveillance for advanced prostate cancer (3). Therefore, novel approaches and agents are urgently needed for the prevention and treatment of prostate carcinoma. High throughput technologies, such as DNA and protein microarrays, have enabled the identification of genes and their corresponding proteins that are differentially regulated in malignant conditions (4).

Mediator complex subunit 19 (MED19) is a component of the mediator complex which is a coactivator for DNA-binding factors that activate transcription via RNA polymerase II (5). It was originally identified in a search for mutants that increased the aerobic expression of the *CYC7* gene, and was initially found to be encoded by an essential gene product (6). Gene expression microarray studies of a MED19 deletion strain and a truncation strain have shown that a diverse range of genes were both up- and down-regulated (7). MED19 was involved in head-module subunits in mammalian mediator complex (8). The largely intact *Δmed19(rox3)* complex facilitates activated transcription at levels similar to the wild type mediator; However, in the absence of the middle module, the *Δmed19(rox3)* mediator was defective in enhanced basal transcription, enhanced transcription factor II H (TFIIH) phosphorylation of the carboxy terminal domain (CTD), as well as binding of RNA Pol II and the CTD (9). Recently, MED19 was identified as one of critical components of the regulatory apparatus employed by the repressor element 1 (RE1) silencing transcription factor (10).

MED19 encodes lung cancer metastasis-related protein (LCMR1) in human genome (11, 12). Its functional role in human prostate cancer is still unclear. Loss of either MED1/TRAP220 or MED17 in prostate cancer cells significantly decreased both androgen-dependent and -independent cellular proliferation, inhibited cell cycle progression, and increased apoptosis (13). Hence, we hypothesized that MED19 was involved in the transportation of cell signals from the exterior to the interior of the nucleus, cell cycle regulation, and the regulation of transcription in carcinomas.

To explore the functional role of MED19 in prostate cancer, we performed the infection into PC-3 and DU145 cells with lentivirus expressing short harpin RNA (shRNA) against MED19, and investigated the effect of MED19 silencing on the cell proliferation, tumorigenesis cell cycle, and apoptosis.

RESULTS

Infection of lentivirus containing shRNA targeting MED19 in PC-3 cells

To assess the role of MED19 in prostate carcinoma, we synthe-

*Corresponding author. Tel: 86-21-81885732; Fax: 86-21-81885732; E-mail: danfengxu@yeah.net
http://dx.doi.org/10.5483/BMBRep.2011.44.8.547

Received 25 January 2011, Accepted 26 May 2011

Keywords: Gene silencing, MED19, Proliferation, Tumorigenesis

sized MED19 siRNA (5′-GGTGAAGGAGAAGCTAAGT-3′) and packaged recombined lentivirus expressing MED19 shRNA (RNAi-1). GFP expression was observed in PC-3 cells 4 days after lentivirus infection at MOI 20 (Fig. 1A). Quantitative real-time (Q-PCR) results showed that the expression of MED19 mRNA was decreased by 75.7% in MED19 knock-down cells, compared to the control ($P < 0.01$; Fig. 1B). Moreover, the expression of MED19 protein was significantly lower after 7 days of RNAi-1 in-

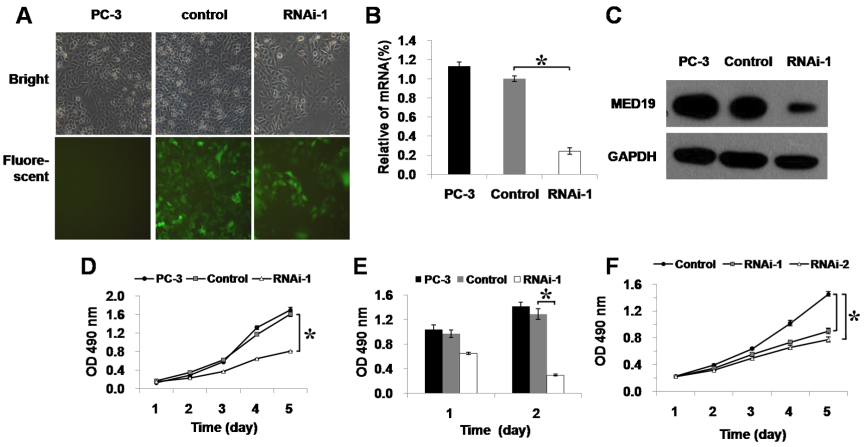

Fig. 1. Silencing of MED19 inhibited the proliferation of PC-3 cells. (A) Representative images of parent cells, control lentivirus infected cells, and RNAi-1 infected cells in bright and fluorescent fields (magnification ×100). (B) The infection with lentivirus containing shRNA targeting MED19 resulted in significant decrease in the expression of MED19 mRNA (*$P < 0.01$). (C) The expression of MED19 protein was significantly lower in the RNAi-1 group than in control as evidenced by Western blot assay. (D) MTT assay: the cell viability was significantly decreased in the RNAi-1 group after 5 days of incubation (*$P < 0.01$). (E) BrdU incorporation assay: The RNAi-1 group showed significant decrease in the DNA synthesis on the second day, indicating a decreased proliferative ability (*$P < 0.01$). (F) The effect of MED19 downregulation on cell proliferation in PC-3 cells was also repeated by using another siRNA against MED19 to get comparable results. The cell viability was significantly lower in the RNAi-1 and RNAi-2 groups than in control (*$P < 0.01$).

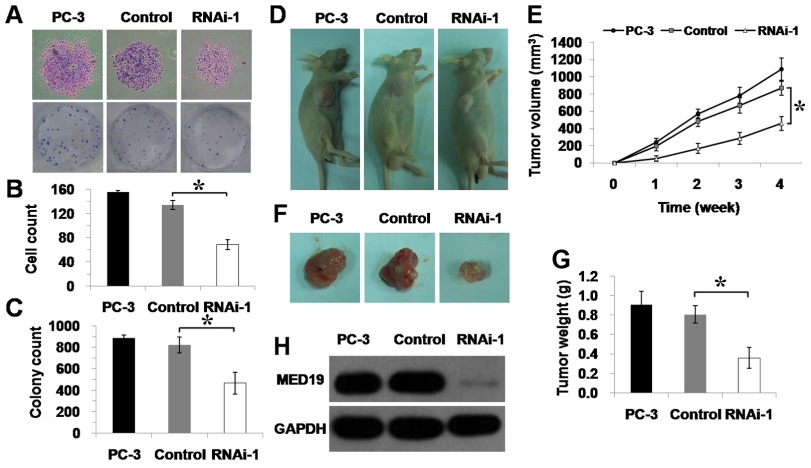

Fig. 2. Silencing of MED19 suppressed the colony-forming capacity and tumorigenesis of PC-3 cells. (A) Images of Giemsa-stained colonies. It revealed that both the number and size of MED19-shRNA derived colonies in each 6-well plate were drastically lower in comparison with the control. (B) Ten colonies were randomly selected to determine the cell count per colony. Compared to the control the number of cells per colony was significantly lower in the RNAi-1 group (*$P < 0.05$). (C) The amount of colonies in the RNAi-1 group was also significantly lower than in the other two groups (*$P < 0.05$). (D) Representative images of nude mice after four weeks of inoculation with PC-3 cells, control infected PC-3 cells, and RNAi-1. Infected PC-3 cells. (E) The growth of tumor in the nude mice xenografts. The tumor growth velocity in the RNAi-1 group was slower than in controls (*$P < 0.01$). (F) The tumors were finally separated, and representative images of tumors were shown. (G) The weight of tumors. There was a significant difference between the control and RNAi-1 group (*$P < 0.05$). (H) The tumor tissue was immuno blotted with a MED19 rabbit polyclonal antibody. The expression level of MED19 protein was significantly lower in the RNAi-1 group than in controls ($P < 0.05$).

fection (Fig. 1C), demonstrating that MED19 was efficiently downregulated in PC-3 cells by lentivirus-mediated shRNA.

Suppression of MED19 inhibited the growth of PC-3 cells

After infection with RNAi-1 for 5 days, MTT and BrdU incorporation assay were used to assess the effect of MED19 silencing on cell proliferation in PC-3 cells. Compared to the control, the number of viable cells was reduced by 49.7% after 5 days of incubation in RNAi-1 group ($P < 0.01$; Fig. 1D), and the level of newly synthesized DNA was decreased by 76.9% on the second day ($P < 0.01$; Fig. 1E), which indicated a impaired proliferative ability in PC-3 cells. To rule out off-target effects caused by the siRNA, relevant data was also confirmed with an additional RNAi sequence (5′-CGAATCTGATCACACACTA-3′) that deplete MED19 and inhibited cell proliferation with a similar efficiency (Fig. 1F).

Silencing of MED19 suppresses the colony-forming capacity and tumorigenesis of PC-3 cells

Giemsa stained colonies in Fig. 2A revealed that stable infection of RNAi-1 resulted in dramatic decrease in the number and size of colonies. Compared to the control, the cell number per colony and colony count per well were reduced by 43.0% and 51.0% in RNAi-1 group, respectively ($P < 0.05$; Fig. 2B and C). To investigate the *in vivo* effect of MED19 shRNA, on tumorigenesis a prostate carcinoma xenograft model was established (Fig. 2D). Four weeks of inoculation, the average tumor volume was 2.4-fold and 1.9-fold larger in PC-3 group and control group than in RNAi-1 group ($P < 0.05$; Fig. 2E). Tumor xenografts were finally separated (Fig. 2F), and a significant different in the tumor weight was observed between control and RNAi-1 groups ($P < 0.05$; Fig. 2G). Moreover, the expression of MED19 in tumors from RNAi-1 group was significantly lower than in control (Fig. 2H). Our *in vivo* results revealed that silencing of MED19 suppressed the tumor formation and growth in prostate cancer cells.

Effect of MED19 downregulation on the growth of DU145 cells

The silencing of MED19 in another prostate cancer line, DU145 cells, was substantiated by Western blotting (Fig. 3A). The cell proliferation was significantly inhibited after 5 days of RNAi-1 infection as evidenced by MTT assay ($P < 0.01$; Fig. 3B). Moreover, thecolony count was proved to be only 30.5% smaller in MED19 knock-down cells than in control ($P < 0.01$; Fig. 3C, D). In conclusion, lentivirus-mediated MED19 shRNA impaired the cell proliferation and colony formation in DU145 cells.

Effect of MED19 downregulation on the cell cycle and apoptosis

Flow cytometry assay was performed to further assess the role of MED19 in the regulation of cell cycle progression and apoptosis. Compared to the control, the proportion of S-phase cells was increased by 47.0% and 23.7% in RNAi-1 infected PC-3 cells and DU-145 cells (Fig. 4A, B). This demonstrates that MED19 knockdown cells underwent significant S-phase arrest. Next, we wanted to determine whether MED19 was an inducer of apoptosis. The apoptosis profile was different between the control group and RNAi groups (Fig. 4C). Cell apoptosis induced by MED19 siRNAs was significantly increased in comparison with control (Fig. 4D), indicating that the growth inhibition was associated

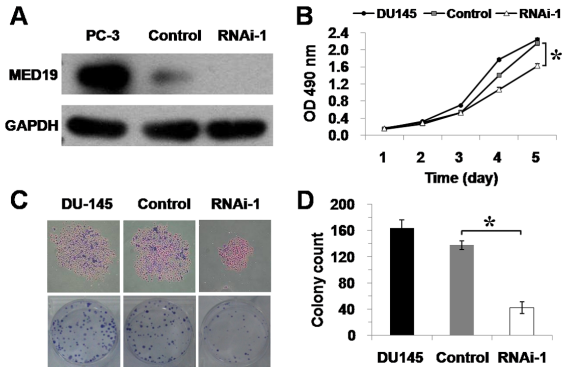

Fig. 3. Silencing of MED19 induced inhibition of cell proliferation in DU145 cells. (A) The expression of MED19 protein was significantly downregulated in DU145 cells that infected with MED19-shRNA-expressing lentivirus for 7 days. (B) Knockdown of MED19 induced cell growth inhibition as evidenced by MTT assay (*$P < 0.01$). (C) After 14 days in culture, each group of DU145 cells were stained with Giemsa. Both the number and size of lentivirus-shRNA derived cell colonies were drastically lower in comparison with control. (D) Colonies of 50 or more cells were counted. It proved that the amount of colonies was significantly lower in RNAi-1 group than control (*$P < 0.01$).

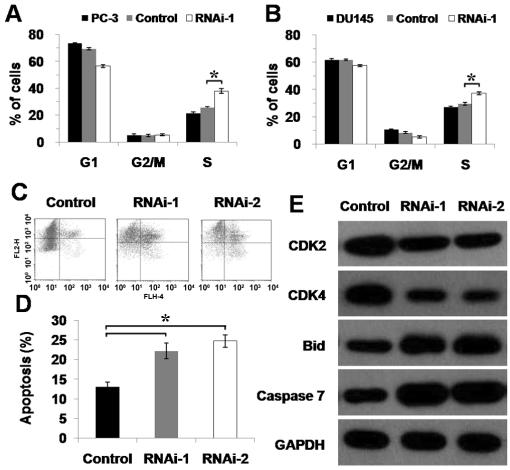

Fig. 4. Silencing of MED19 led to the accumulation of S-phase cells and enhancement of apoptosis. (A, B) Flow cytometric analysis was used to detect the effect of MED19 downregulation on cell cycle distribution in PC-3 cells (A) and DU145 cells (B). The proportion of cells in S phase was significantly higher in the RNAi-1 group than in control, which was accompanied by a decrease in the percentage of cells in G1 phase (*$P < 0.05$). (C, D) PC-3 cells were infected with MED19-shRNA-expressing lentivirus and subjected to Annexin V-PE and 7-AAD apoptosis analysis. The proportion of apoptotic cells was significantly higher in RNAi-1 and RNAi-2 group than in control. (E) Western blot analysis of the downstream target genes of MED19 including CDK2, CDK4, Bid and Caspase 7.

with an increase in cell apoptosis. Furthermore, apoptotic proteins such as Bid, caspase-7 and cell cycle proteins, including CDK2 and CDK4, were measured by Western blotting. We found that CDK2 and CDK4 were downregulated, while Bid and caspase-7 were upregulated significantly (Fig. 4E).

DISCUSSION

MED19 is a member of transcription factors that regulate the gene expression and may be responsible for aberrant of cell growth and tumor formation. So far, the expression of MED19 has not been explored in prostate cancer. In our previous study, we examined the presence of MED19 protein in prostate cancer specimens by immunohistochemical assay. It was suggested that MED19 was specifically highly expressed in the prostate tumor tissues, compared to the paired non-neoplastic tissues (data not shown).

Next, we constructed lentiviruses containing shRNAs targeting MED19 and infected prostate cancer cell lines. The primary goal of this research was to explore the role of MED19 in cell proliferation and tumorigenesis in prostate cancer. After silencing of MED19 by lentivirus-mediated RNAi, the proliferation of PC-3 and DU145 cells was significantly inhibited. Furthermore, infection of lentivirus containing shRNA targeting MED19 resulted in lower colony formation ability and attenuated tumor formation and growth in PC-3 xenografts. This *in vivo* result provided new support for the role of MED19 in promoting neoplasia, which support the results of previous studies that reported an induction of tumorigenesis in hepatocellular carcinoma and lung cancer cells treated with MED19 siRNAs (14, 15). Together, these findings justified the potential usefulness of MED19 as a prostate cancer biomarker.

Abnormal regulation of the cell cycle is a hallmark of carcinoma genesis. In this study, it revealed that PC-3 and DU145 cells were arrested in S-phase when infected with lentiviruse containing shRNA targeting MED19, which suggested that MED19 is involved in control of post-mitotic cellular process. Various studies have shown the involvement of cell cycle regulation-mediated apoptosis as a mechanism of cell growth inhibition (16, 17). In eukaryotes, passage through the cell cycle is governed by the function of a family of protein kinase complexes (18). Under normal conditions, the protein kinase complexes are activated at specific intervals and through a series of events, resulting in the progression of cells through the different phases of the cell cycle, thereby ensuring normal cell growth (19). Any defect in this machinery causes altered cell cycle regulation that may result in unwanted cellular proliferation, potentially culminating in the development of cancer. CDK2 and CDK4, subunits of the protein kinase complex, are involved in cell cycle regulation (G1 to S transition). Interestingly, our data showed that CDK2 and CDK4 was downregulated in PC-3 cells, which maybe not consistent with the S phase arrest after MED19 siRNA treatment observed by flow cytometry. Similar to our results, in a human hepatocellular carcinoma cells line, the cell cycle was also arrested in the S phase by decreasing CDK4 protein expression (20) However, further investigation is desirable to reveal the underlying mechanism by which MED19 modulates the cell cycle.

Our results also showed that knocking down MED19 caused upregulation of apoptotic caspase Caspase 7 and pro-apoptotic protein Bid, which results in enhancement of cell apoptosis. Moreover, MED19 knock-down cells may be dying a programmed cell death with undergoing an S-phase arrest.

In conclusion, downregulation of endogenous MED19 induces growth inhibition, S-phase arrest, apoptosis, and changes in cell cycle and apoptosis regulators in prostate cancer cells. MED19 acts as a carcinogene and might be useful as an adjunctive therapeutic agent for advanced prostate cancer. A better understanding of MED19 function and processing may provide novel insights into the clinical therapy of prostate cancer.

MATERIALS AND METHODS

Cell culture

Prostate cancer cell lines PC-3 and DU145 were obtained from the American Type Culture Collection (ATCC, Rockville, MD) and grown in RPMI-1640 supplemented with 10% fetal bovine serum (FBS) and 1 mM nonessential amino acids at 37°C and 5% CO_2.

Lentivirus-mediated RNA interference

The double-strand oligo-DNA containing the small interfering RNAs (siRNAs) against MED19 (NM_153450) or non-silencing siRNA were linked to the linear plasmid pGCL-GFP (Shanghai GeneChem, China). The production of recombinant plasmids afterwards were transfected into HEK293T cells together with helper plasmids (all obtained from Shanghai GeneChem) using Lipofectinmine 2000 (Invitrogen, Carlsbad, CA) to generate lentiviruses. After 72 h of transfection, lentiviruse particles were harvested and concentrated by ultracentrifugation. PC-3 and DU145 cells were seeded at 6-well plates (5×10^4 cells/ml) and infected with lentiviruses containing shRNAs targeting MED19 or control lentivirus at multiplicity of infection (MOI) of 20.

Q-PCR

After 5 days of infection, total cellular RNA was extracted with Trizol reagents (Invitrogen, Carlsbad, CA) and corresponding first-strand cDNA was synthesized using M-MLV-RTase (Promega, Madison, WI) according to the manufacturer's protocols. The amount of MED19 mRNA knock-down was quantified by employing Q-PCR using the ABI PRISM 7700 Sequence Detection System (Applied Biosystems, Foster City, CA). The primer sequences for MED19 were: 5′-TGACAGGCAGCACGAATC-3′ and 5′-CAGGTCAGGCAGGAAGTTAC-3′. The primer sequences for GAPDH, an internal control, were 5′-TGACTTCAACAGCGACACCCA-3′ and 5′-CACCCTGTTGCTGTAGCCAAA-3′. Relative expression of MED19

mRNA was calculated using 2-$\Delta\Delta$Ct method (21).

Western blot analysis

After 7 days of infection, cells were homogenized in NP-40 lysis buffer containing 50 mM Tris-HCl (pH 7.4), 1% NP-40 (Sigma, St, Louis, MO) and complete protease inhibitor cocktail (Roche, Indianapolis, IN). Protein extracts (15 μg) was mixed with SDS sample buffer and run on a 10% SDS-polyacrylamide gel. The separated proteins were transferred onto polyvinylidene fluoride membranes, which were incubated for 1 h in blocking buffer (Tris-buffered saline with 0.05% Tween [TBS-T] and 5% non-fat dry milk). MED19 rabbit polyclonal antibody (Abcam, Cambridge, MA) was applied at 1 : 5,000 in blocking buffer overnight at 4°C. After washing with TBS-T buffer, the membrane was further incubated with a horseradish peroxidase-conjugated goat anti-rabbit IgG antibody (Santa Cruz Biotechnology, Santa Cruz, CA) at 1 : 5,000 for 1 h at room temperature. GAPDH was used as a loading control. The signals were visualized with the ECL detection system (GE Healthcare, Piscataway, NJ) and autoradiography. For analysis of CDK2, CDK4, Bid, and Caspase 7 protein, membranes were blocked and probed with anti-CDK4 antibody (Sigma, St. Louis, MO), anti-CDK2 antibody (Sigma, St. Louis, MO), Bid antibody (Abcam, Cambridge, MA), and Caspase-7 antibody (Cell Signaling Technology, Beverly, MA), respectively.

Cell proliferation assay

Cell viability was assessed by MTT assay 5 days after lentivirus infection (22). Briefly, cells were seeded into 96-well plates (2×10^4 cells/ml) and allowed to grow for 5 days, respectively. Twenty microliter (5 mg/ml) of MTT was added and incubated for 4 h. The supernatant was removed and 150 μl DMSO was added. The optical density (OD) of each well was measured at 570 nm.

The DNA synthesis ability was measured by BrdU incorporation assay (22). Briefly, cells were seeded into 96-well plates (2×10^4 cells/ml) and allowed to grow for 2 days. BrdU Cell Proliferation Assay Kit (Chemicon International Inc., Temecula, CA) was used, and the OD of each well was measured at 490 nm.

Colony formation analysis

Colony formation analysis was conducted 5 days after lentivirus infection as previously described (22). Cells were seeded into 6-well plates (300 cells/ml) and cultured normally for 14 days. Then colonies were washed with PBS twice, fixed in paraform and stained with Giemsa. The number of colonies was counted under fluorescence microscope.

Cell cycle analysis

After lentivirus infection for 5 days, cells were spread onto 60-mm tissue culture dishes and incubated to reach 80% confluence. Then, cells were fixed in 70% ice-cold ethanol and stained with propidium iodide (40 μg/ml) in RNase (100 μg/ml). Tests were performed in triplicate for each sample. Analysis of cell cycle distribution was performed on a flow cytometer (FACS Calibur, BD, Franklin, NJ) with dedicated software.

Apoptosis assay

The Annexin V-PE and 7-AAD double staining flow cytometry apoptosis detection kit (BD Biosciences, San Jose, CA) was used according to the manufacturer's suggestions. Briefly, PC-3 cells grown in 60-mm tissue culture dishes were infected with lentivirus for 7 days. Both floating and attached cells were collected in PBS and centrifuged. The supernatant was discarded and the pellets were resuspended in binding buffer at 1×10^6 cells/ml. After incubation with the dye for 15 min, cells were analysed on a FACSCalibur flow cytometer.

Assessment of tumor growth

Thirty male BALB/c nude mice (4-6 weeks old, 18-22 g) were purchased from Shanghai Slac Laboratory Animal Co., Ltd. and randomly divided into three groups (each containing 10 mice). The study protocol was reviewed and approved by the Institutional Animal Care and Use Committee of the Second Military Medical University. Animals received a subcutaneous injection of 0.15 ml of parent PC-3 cells or lentivirus infected cells (5×10^6 cells/ml). Tumor growth was assessed on an indicated interval by measuring tumor size with digital calipers. The formula: $0.52 \times a^2 \times b$, where a = minor diameter and b = major diameter, was used to calculate the tumor volume. Tumors were dissected and weighed 4 weeks after inoculation and subjected to Western blotting.

Statistical analysis

Data were expressed as mean ± SD and were statistically analyzed using unpaired Student's *t* test or ANOVA analysis with the SPSS 10.0 statistical package. $P < 0.05$ was considered statistically significant.

Acknowledgments

The authors are thankful for the financial support from National Natural Science Foundation of China for Youths (No. 81001136), National Natural Science Foundation of China (No. 30973006) and Shanghai Committee of Science and Technology General Program for Medicine (No. 10411963600).

REFERENCES

1. Grönberg, H. (2003) Prostate cancer epidemiology. *Lancet* **361**, 859-864.
2. Jemal, A., Siegel, R., Ward, E., Murray, T., Xu, J. and Thun, M. J. (2007) Cancer statistics. *CA Cancer J. Clin.* **57**, 43-66.
3. Walczak, J. R. and Carducci, M. A. (2007) Prostate cancer: a practical approach to current management of recurrent disease. *Mayo. Clin. Proc.* **82**, 243-249.
4. Dhanasekaran, S. M., Barrette, T. R., Ghosh, D., Shah, R., Varambally, S., Kurachi, K., Pienta, K. J., Rubin, M. A. and Chinnaiyan, A. M. (2001) Delineation of prognostic biomarkers in prostate cancer. *Nature* **412**, 822-826.

5. Sato, S., Tomomori-Sato, C., Banks, C. A., Parmely, T. J., Sorokina, I., Brower, C. S., Conaway, R. C. and Conaway, J. W. (2003) A mammalian homolog of Drosophila melanogaster transcriptional coactivator intersex is a subunit of the mammalian Mediator complex. *J. Biol. Chem.* **278**, 49671-49674.
6. Rosenblum-Vos, L. S., Rhodes, L., Evangelista, C. C. Jr., Boayke, K. A. and Zitomer, R. S. (1991) The ROX3 gene encodes an essential nuclear protein involved in CYC7 gene expression in Saccharomyces cerevisiae. *Mol. Cell Biol.* **11**, 5639-5647.
7. Becerra, M., Lombardía-Ferreira, L. J., Hauser, N. C., Hoheisel, J. D., Tizon, B. and Cerdán, M. E. (2002) The yeast transcriptome in aerobic and hypoxic conditions: effects of hap1, rox1, rox3 and srb10 deletions. *Mol. Microbiol.* **43**, 545-555.
8. Conaway, R. C., Sato, S., Tomomori-Sato, C., Yao, T. and Conaway, J. W. (2005) The mammalian Mediator complex and its role in transcriptional regulation. *Trends Biochem. Sci.* **30**, 250-255.
9. Baidoobonso, S. M., Guidi, B. W. and Myers, L. C. (2007) MED19 (Rox3) regulates Intermodule interactions in the Saccharomyces cerevisiae mediator complex. *J. Biol. Chem.* **282**, 5551-5559.
10. Ding, N., Tomomori-Sato, C., Sato, S., Conaway, R. C., Conaway, J. W. and Boyer, T. G. (2009) MED19 and MED26 are synergistic functional targets of the RE1 silencing transcription factor in epigenetic silencing of neuronal gene expression. *J. Biol. Chem.* **284**, 2648-2656.
11. Gustafsson, C. M., Myers, L. C., Li, Y., Redd, M. J., Lui, M., Erdjument-Bromage, H., Tempst, P. and Kornberg, R. D. (1997) Identification of Rox3 as a component of mediator and RNA polymerase II holoenzyme. *J. Biol. Chem.* **272**, 48-50.
12. Sato, S., Tomomori-Sato, C., Parmely, T. J., Florens, L., Zybailov, B., Swanson, S. K., Banks, C. A., Jin, J., Cai, Y., Washburn, M. P., Conaway, J. W. and Conaway, R. C. (2004) A set of consensus mammalian mediator subunits identified by multidimensional protein identification technology. *Mol. Cell* **14**, 685-691.
13. Vijayvargia, R., May, M. S. and Fondell, J. D. (2007) A coregulatory role for the mediator complex in prostate cancer cell proliferation and gene expression. *Cancer Res.* **67**, 4034-4041.
14. Zou, S. W., Ai, K. X., Wang, Z. G., Yuan, Z., Yan, J. and Zheng, Q. (2011) The role of Med19 in the proliferation and tumorigenesis of human hepatocellular carcinoma cells. *Acta. Pharmacol. Sin.* **32**, 354-360.
15. Sun, M., Jiang, R., Li, J. D., Luo, S. L., Gao, H. W., Jin, C. Y., Shi, D. L., Wang, C. G., Wang, B. and Zhang, X. Y. (2011) MED19 promotes proliferation and tumorigenesis of lung cancer. *Mol. Cell Biochem.* DOI: 10.1007/s11010-011-0835-0.
16. Malik, A., Afaq, F., Sarfaraz, S., Adhami, V. M., Syed, D. N. and Mukhtar, H. (2005) Pomegranate fruit juice for chemoprevention and chemotherapy of prostate cancer. *Proc. Natl. Acad. Sci.* **102**, 14813-14818.
17. Sarfaraz, S., Afag, F., Adhami, V. M., Malik, A. and Mukhtar, H. (2006) Cannabinoid receptor agonist-induced apoptosis of human prostate cancer cells LNCaP proceeds through sustained activation of ERK1/2 leading to G1 cell cycle arrest. *J. Biol. Chem.* **281**, 39480-39491.
18. Ahmad, N., Feyes, D. K., Agarwal, R. and Mukhtar, H. (1998) Photodynamic therapy results in induction of WAF1/CIP1/P21 leading to cell cycle arrest and apoptosis. *Proc. Natl. Acad. Sci.* **95**, 6977-6982.
19. Sanchez, G., Coronado, X., Zulantay, I., Apt, W., Gajardo, M., Solari, S. and Venegas, J. (2005) Monitoring the efficacy of specific treatment in chronic chagas disease by polymerase chain reaction and flow cytometry analysis. *Parasite* **12**, 353-357.
20. Li, Z. F., Wang, Z. D., Ji, Y. Y., Zhang, S., Huang, C., Li, J. and Xia, X. M. (2009) Induction of apoptosis and cell cycle arrest in human HCC MHCC97H cells with Chrysanthemum indicum extract. *World J. Gastroenterol.* **15**, 4538-4546.
21. Varambally, S., Laxman, B., Mehra, R., Cao, Q., Dhanasekaran, S. M., Tomlins, S. A., Granger, J., Vellaichamy, A., Sreekumar, A., Yu, J., Gu, W., Shen, R., Ghosh, D., Wright, L. M., Kladney, R. D., Kuefer, R., Rubin, M. A., Fimmel, C. J. and Chinnaiyan, A. M. (2008) Golgi protein GOLM1 is a tissue and urine biomarker of prostate cancer. *Neoplasia* **10**, 1285-1294.
22. Xu, Y., Wang, Z., Wang, J., Li, J., Wang, H. and Yue, W. (2010) Lentivirus-mediated knockdown of cyclin Y (CCNY) inhibits glioma cell proliferation. *Oncol. Res.* **18**, 359-364.